Reference quiet-Sun Lyman-α and Mg II h&k line profiles as a boundary condition for radiative transfer modelling of the solar atmosphere

S. Gunár[1], P. Schwartz[2], J. Koza[2], P. Heinzel[1] and W. Liu[1]

Astronomický ústav AV ČR

[1] Astronomical Institute of the Czech Academy of Sciences, 25165 Ondřejov, Czech Republic

[2] Astronomical Institute of the Slovak Academy of Sciences, 05960 Tatranská Lomnica, Slovakia

Astronomický ústav SAV

Using the best sets of Lyman-α and Mg II h&k solar-disk observations currently available, we derived reference quiet-Sun profiles of Lyman-α and Mg II h&k lines representing solar radiation during a minimum of solar activity. These profiles can serve as an incident radiation boundary condition for the radiative transfer modelling of chromospheric and coronal structures for which the illumination in Lyman-α and Mg II h&k lines plays a significant role. The solar radiation in these strong lines is important also for the investigation of the heliosphere, Earths ionosphere, and the atmospheres of planets, moons, and comets.

To derive the Lyman-α reference profile (Fig. 3), we used eight SOHO/SUMER raster scans (Fig. 1) obtained without the use of the attenuator. These observations were performed in various quiet-Sun regions on three consecutive days during a period of minimum solar activity. A detailed analysis of all eight SOHO/SUMER rasters does not show any clear evidence of a centre-to-limb variation in the Lyman-α integrated intensities (Fig. 2). That is in agreement with the findings of Curdt et al. (2008).

Solar radiation in Lyman lines is not constant over time but varies significantly with the solar cycle. To take these changes into account, we developed a method that uses the LISIRD composite Lyman-α index (Machol et al. 2019) to adapt the intensities of Lyman-α and higher Lyman lines to a specific date. As is clear from Fig. 4, differences between the total Lyman-α irradiance during maxima and minima of the solar cycle can reach up to 100%. These differences remain high (up to 50%) even after applying a 400-days running average to the index.

To estimate the influence of the change in the incident radiation in the Lyman lines on the results of radiative transfer models, we used the 2D prominence fine structure model of Heinzel & Anzer (2001). The analysis of the influence of the change in the incident radiation shows that the synthetic spectra are strongly affected by modification of the incident radiation boundary condition (see Table 1). The most pronounced impact is on the central and integrated intensities of the Lyman lines. There, the change in the synthetic spectra can often have the same amplitude as the change in the incident radiation itself. The impact on the specific intensities in the peaks of reversed Lyman-line profiles is smaller but still significant. The hydrogen Hα line can also be considerably affected, even though the Hα radiation from the solar disk does not vary with the solar cycle.

More details can be found in Gunár et al. (2020), together with datasets describing the reference Lyman-α profile and the variation of the Lyman lines with the solar cycle throughout the lifetime of SOHO. The LISIRD composite Lyman-α index is accessible at: `lasp.colorado.edu/lisird/data/composite_lyman_alpha`.

Fig. 1. We use eight SOHO/SUMER Lyman-α raster scans obtained on Jun 24, Jun 25, and Jun 26, 2008. Rasters have dimensions of 120″ × 120″ and consist of 80 slit positions.

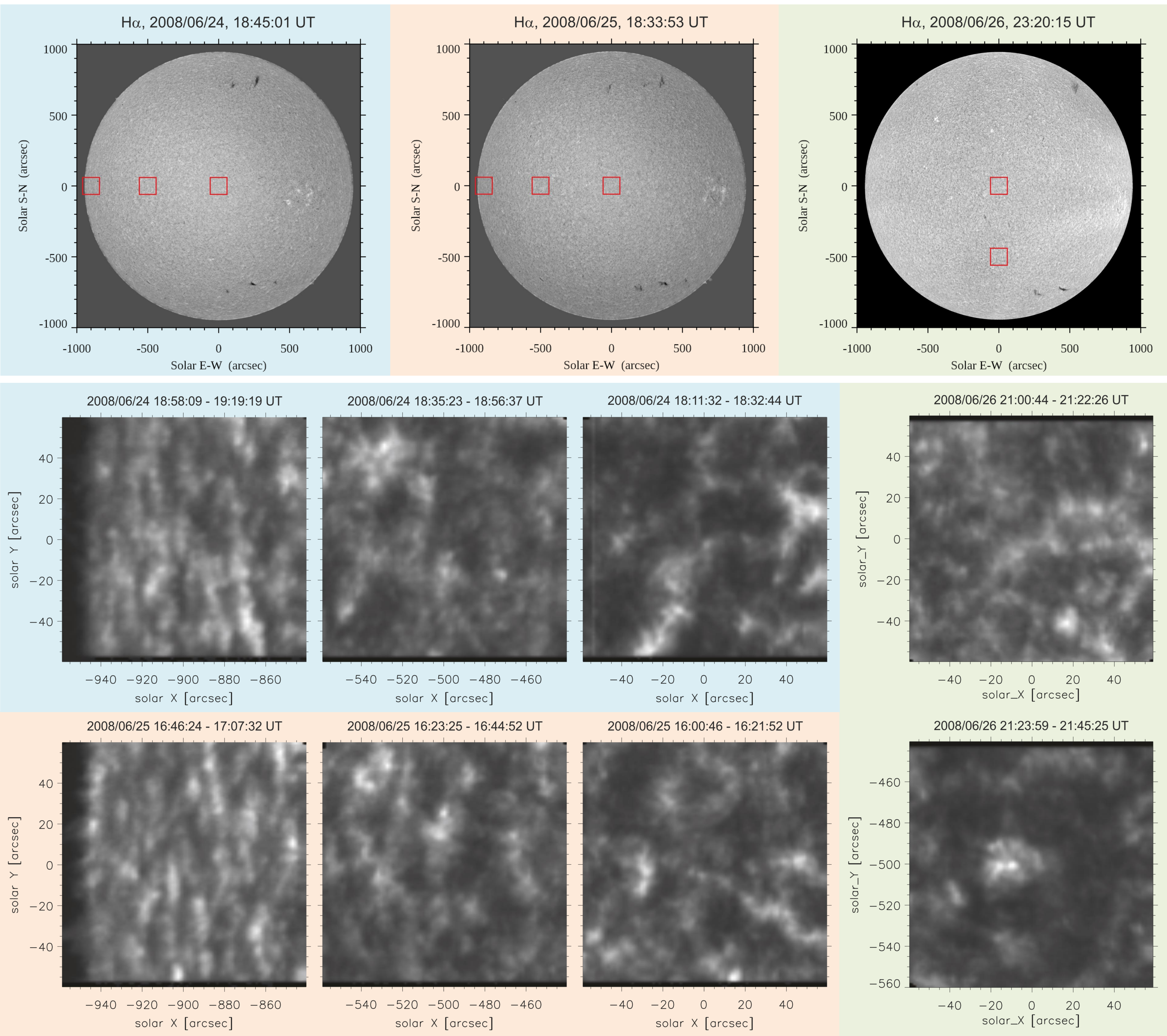

Fig. 2. Centre-to-limb variation: Averaging the Lyman-α integrated intensities from all rasters over concentric arcs with a width of 1″ (each arc is represented by a circle) does not show any clear trend.

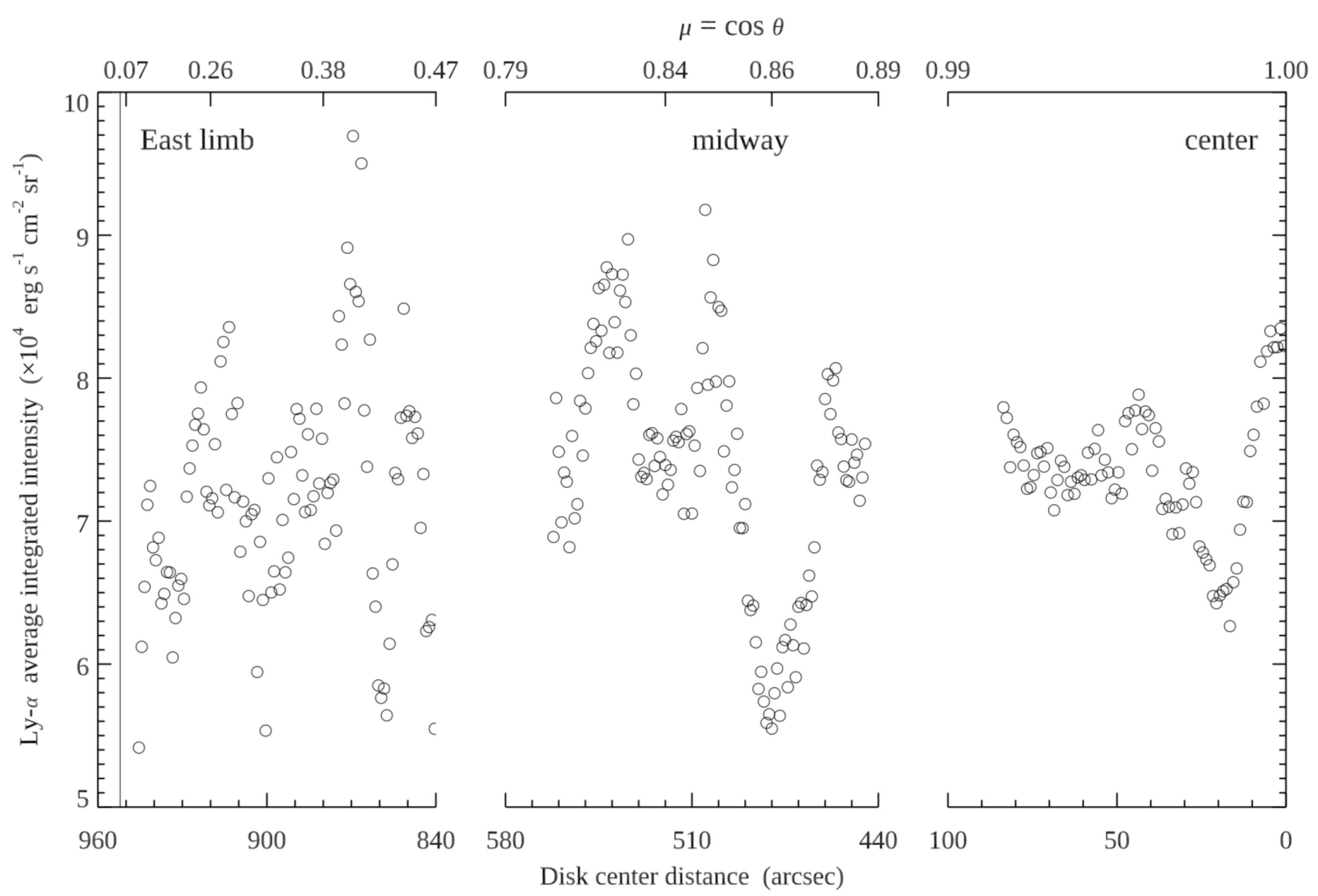

Fig. 4. The variation of the total Lyman-α irradiance based on the LISIRD composite Lyman-α index (grey line) smoothed by the running average over 400 days (red line).

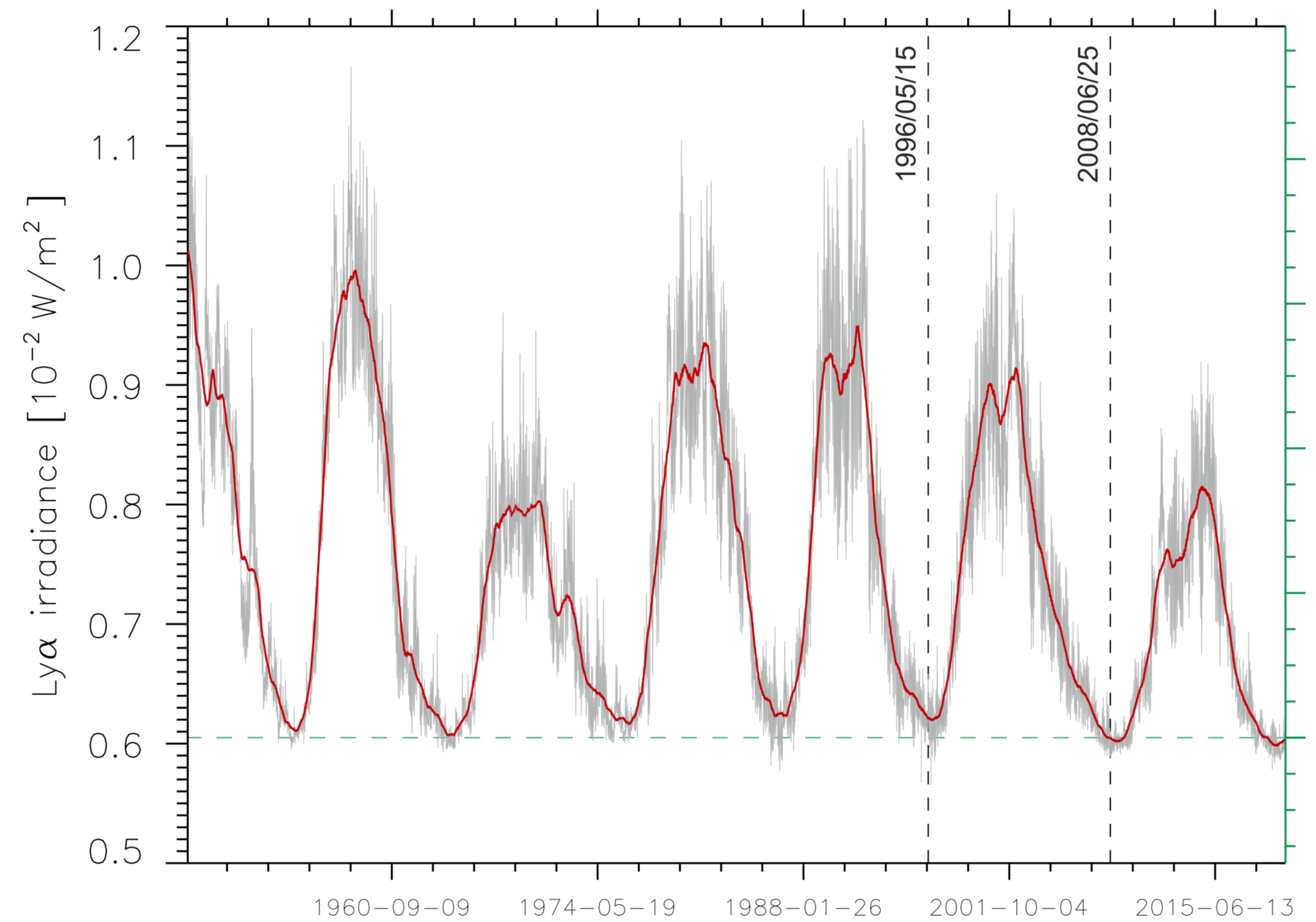

Fig. 3. The reference quiet-Sun Lyman-α profile obtained as an average over all rasters. The grey area indicates the uncertainty estimated to be $\pm(15/\sqrt{3})$%.

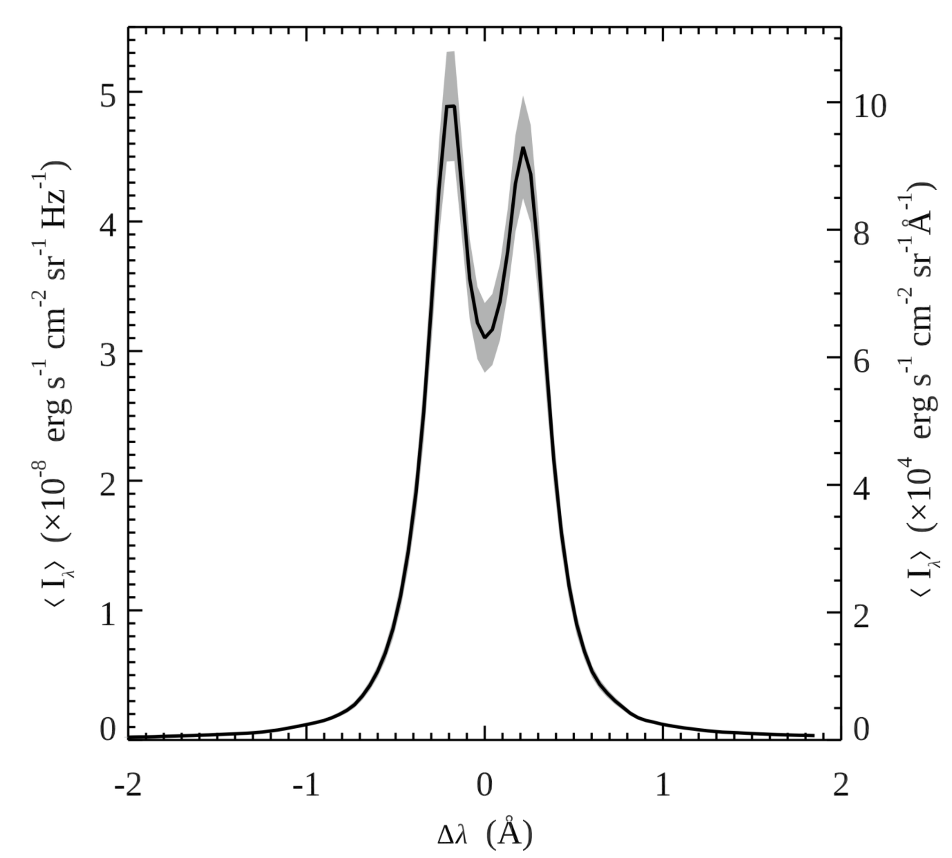

Tab. 1. Relative differences between central, integrated, and peak intensities of the synthetic spectra obtained for selected dates and those obtained for the reference date Jun 25, 2008.

Inc. rad difference	Date	Lyman-α intensity			Lyman-β intensity			Lyman-γ intensity			Hα intensity		
		centre	integral	peak	centre	integral	peak	centre	integral	peak	centre	integral	
7 %	2010/06/24	7 %	6 %	5 %	6 %	6 %	3 %	6 %	6 %	2 %	3 %	3 %	max
		6 %	5 %	2 %	5 %	3 %	1 %	3 %	2 %	1 %	1 %	1 %	median
		6 %	2 %	-	2 %	1 %	-	1 %	1 %	-	-	-	min
12 %	2011/01/01	11 %	11 %	7 %	10 %	10 %	5 %	10 %	9 %	4 %	5 %	5 %	max
		10 %	9 %	3 %	8 %	5 %	2 %	5 %	3 %	2 %	2 %	2 %	median
		10 %	3 %	1 %	3 %	2 %	1 %	1 %	1 %	1 %	-	-	min
20 %	2011/06/24	19 %	18 %	13 %	18 %	17 %	9 %	16 %	16 %	6 %	8 %	9 %	max
		17 %	15 %	5 %	14 %	8 %	4 %	9 %	5 %	3 %	4 %	3 %	median
		16 %	5 %	1 %	6 %	4 %	1 %	2 %	2 %	2 %	-	-	min
26 %	2013/06/24	25 %	24 %	17 %	24 %	22 %	13 %	22 %	21 %	9 %	11 %	11 %	max
		23 %	20 %	7 %	19 %	11 %	5 %	12 %	7 %	4 %	5 %	5 %	median
		22 %	6 %	2 %	8 %	5 %	2 %	3 %	3 %	3 %	1 %	-	min
34 %	2014/06/24	33 %	32 %	22 %	31 %	29 %	16 %	29 %	28 %	11 %	14 %	15 %	max
		30 %	26 %	10 %	25 %	15 %	7 %	16 %	9 %	6 %	6 %	6 %	median
		29 %	8 %	3 %	11 %	7 %	2 %	4 %	3 %	3 %	1 %	-	min

To derived high-precision reference profiles of the Mg II h&k lines (Fig. 6) representing the quiet Sun during a minimum of the solar activity, we used the broad catalogue of IRIS full-Sun mosaics. To minimize the influence of the local variations due to the on-disk solar features and to achieve low levels of uncertainties, we used 12 IRIS full-Sun mosaics without sunspots or other significant signs of solar activity.

The limb darkening – a progressive decrease of intensity with the shortening distance from the solar limb – is clearly visible in the Mg II h&k lines. To properly characterize this variation, we divided IRIS full-Sun mosaics into 10 zones (*a* - *j*) consisting of concentric rings with an equal area (Fig. 5). When plotted side-by-side, Mg II k line profiles from individual zones clearly show the gradual decrease of the intensities going from the disk-centre zone *a* to the near-limb zone *j*. In Figure 8, we show the integrated intensities of the Mg II h and MgII k lines as a function of distance from the disk centre. In the case of 3.5 Å wide range, the intensities in the near-limb zone j are lower by about 35% than those in the disk-centre zone a. The difference in the case of 1.0 Å wide range is around 23%.

Fig. 5. We use 12 IRIS full-Sun mosaics devided into 10 zones (*a* - *j*) with an equal area. The mosaics were obtained between Apr 2019 and Sept 2020 on days without sunspots or other significant signs of solar activity.

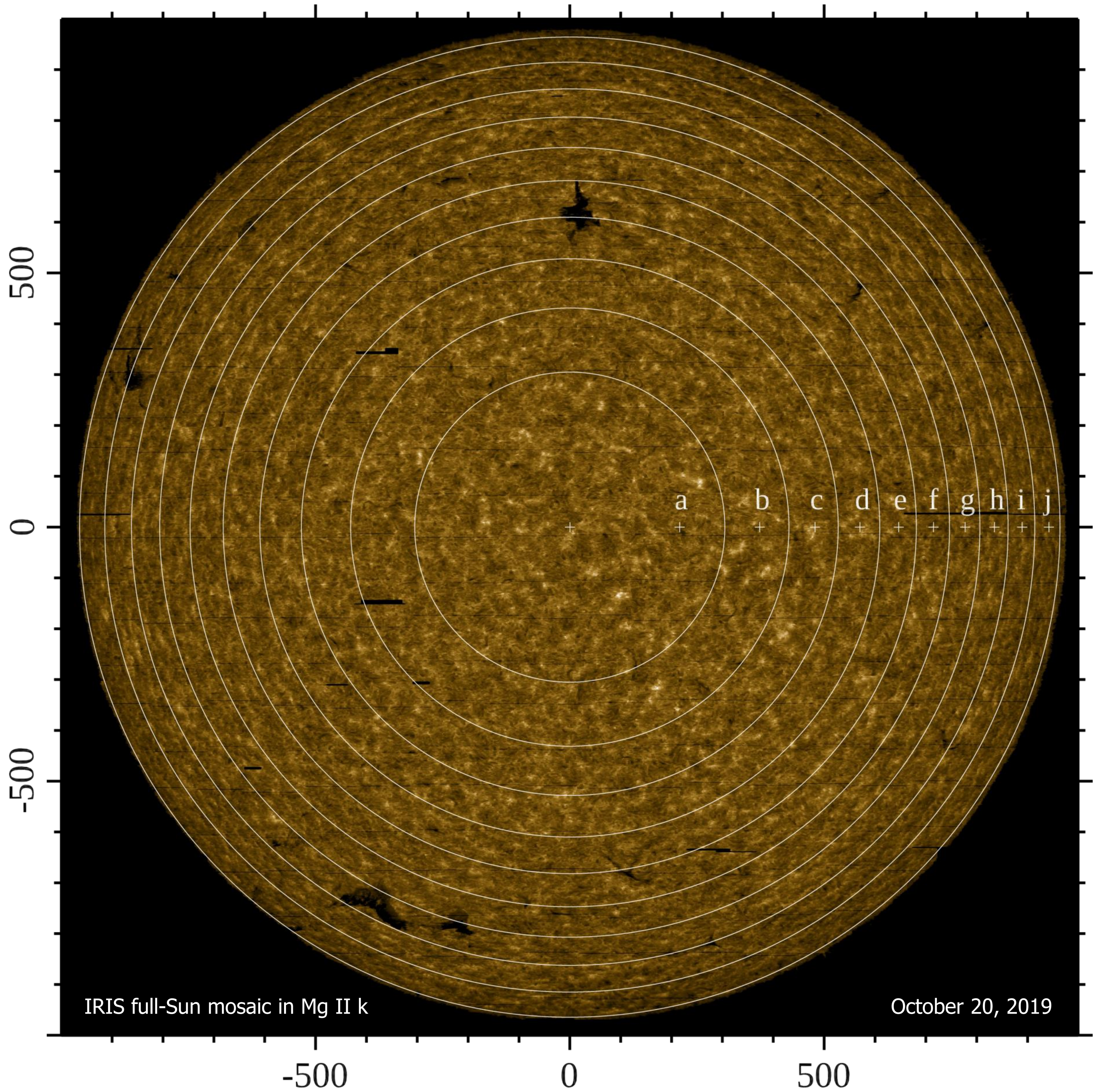

Fig. 7. This composite image of Mg II k profiles averaged over individual zones (*a* - *j*) clearly shows the limb darkening.

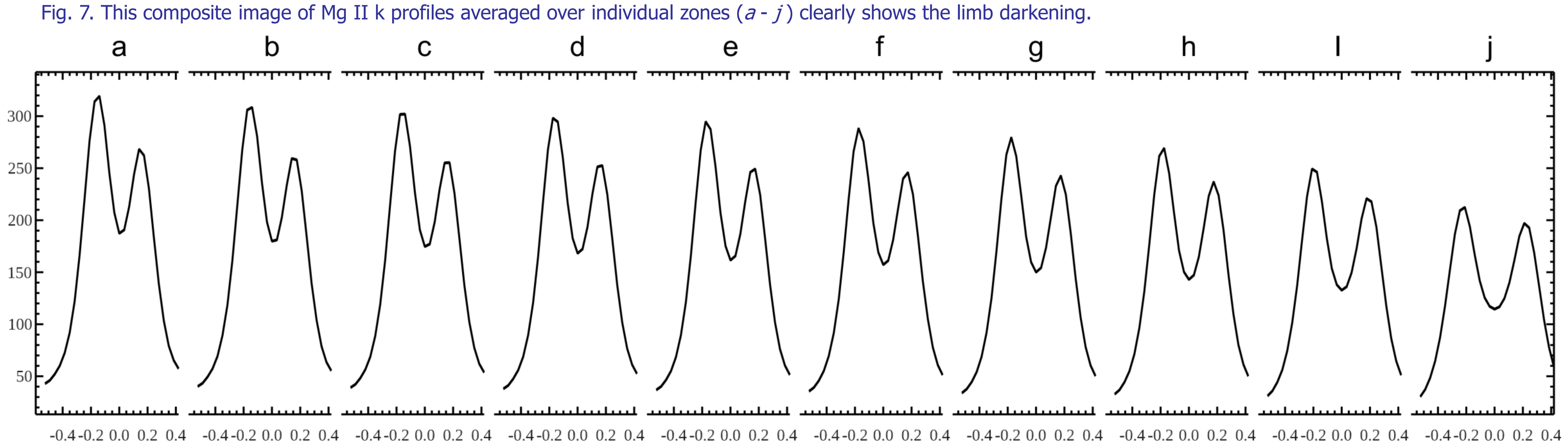

Solar radiation in Mg II h&k lines also changes over time. The extent of its variation can be seen in the observations by SORCE/SOLSTICE shown in Fig. 9, where we display changes in the irradiance of the Mg II k line integrated over ±1.0 Å range. These can reach up to 30%. Even after applying the 400-days running average, differences between minima and maxima of solar activity are about 18%.

Using the 2D prominence model, we analyzed the influence of the change in the incident radiation on the synthetic spectra (see Table 2). The most pronounced impact is on the central and integrated intensities, where the change in the synthetic spectra is often as large as the change in the incident radiation.

More details on the reference Mg II h&k spectra can be found in Gunár et al. (2021a). For details of the variation of the Mg II h&k profiles with the solar cycle see Koza et al. (2021) and poster #150. Our analysis of the impact of the Mg II h&k incident radiation change on the results of the models of the solar atmosphere will be published in Gunár et al. (2021b). The SORCE/SOLSTICE data can be found at `lasp.colorado.edu/lisird/data/sorce_solstice_ssi_high_res`.

Fig. 6. Disk-averaged reference profiles of Mg II k and Mg II h lines. The estimated uncertainties are as low as 2% in the peaks and typically below 10% in the wings of each line.

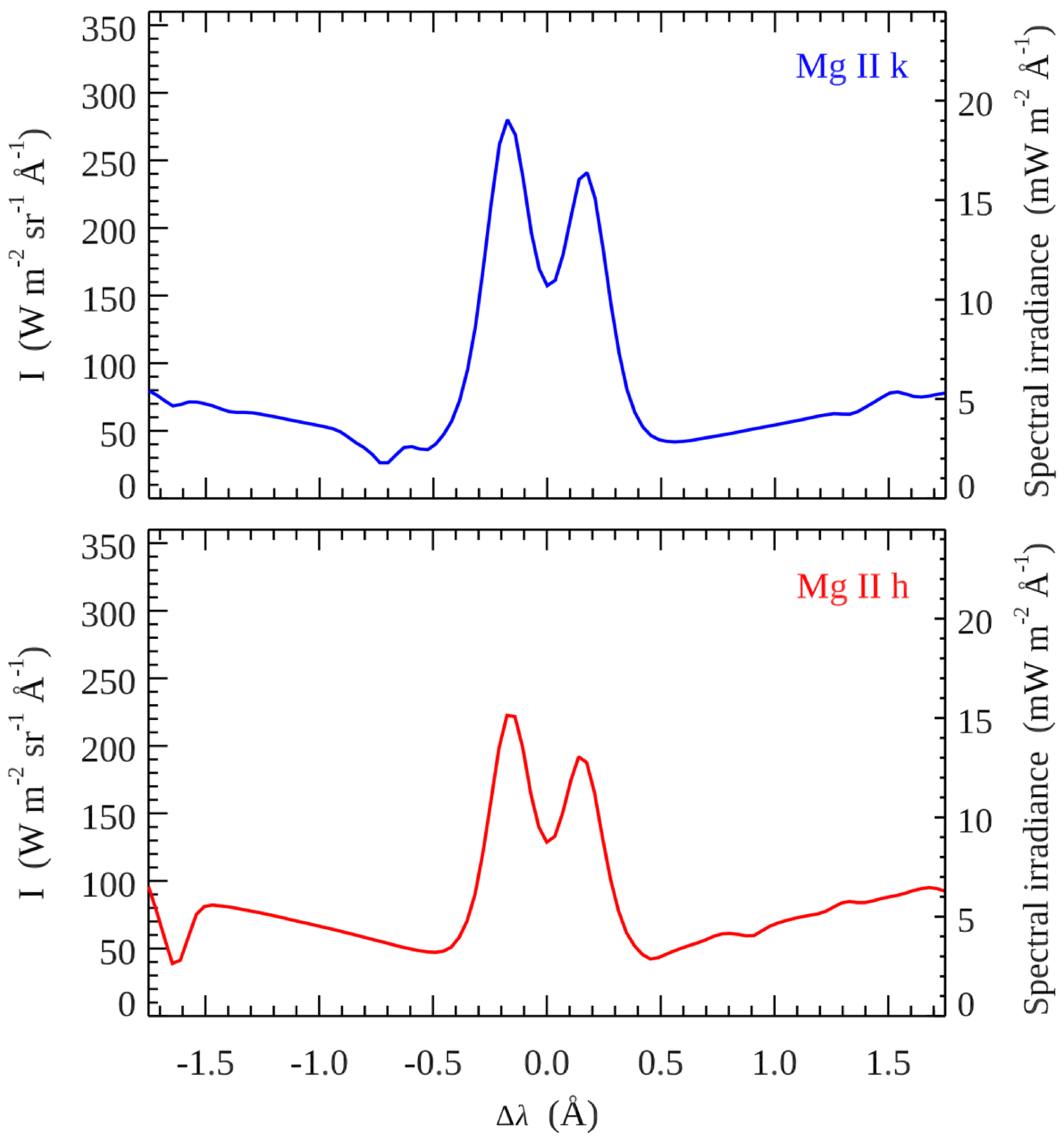

Tab. 2. Relative differences between central, integrated and peak intensities, and the line widths of the synthetic spectra obtained with the Mg II incident radiation increased by 18% and the reference incident radiation data.

Mg II h&k incident radiation change	Mg II h intensity centre	Mg II h intensity integral	Mg II h intensity peak	Mg II h width	Mg II k intensity centre	Mg II k intensity integral	Mg II k intensity peak	Mg II k width	
	17 %	17 %	15 %	0 %	17 %	17 %	15 %	0 %	max
18 %	16 %	16 %	14 %	0 %	16 %	16 %	12 %	0 %	median
	15 %	13 %	13 %	0 %	15 %	12 %	11 %	0 %	min

Fig. 8. Center-to-limb variation of the integrated intensities of the reference Mg II h and Mg II k profiles from individual zones (*a* - *j*). The upper pair of the step functions corresponds to integration over the wavelength range of 3.5 Å while the lower pair corresponds to the integration over 1.0 Å.

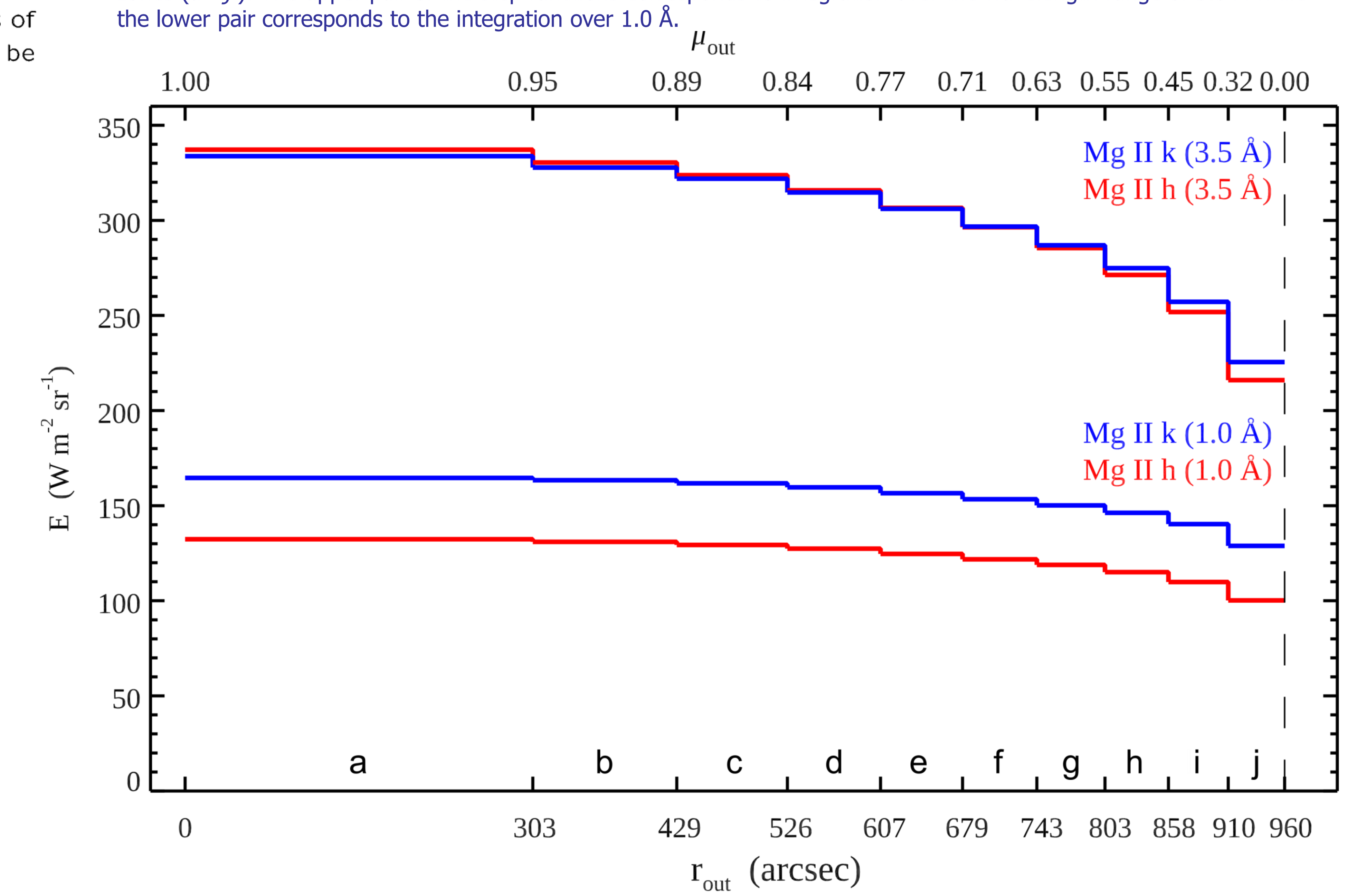

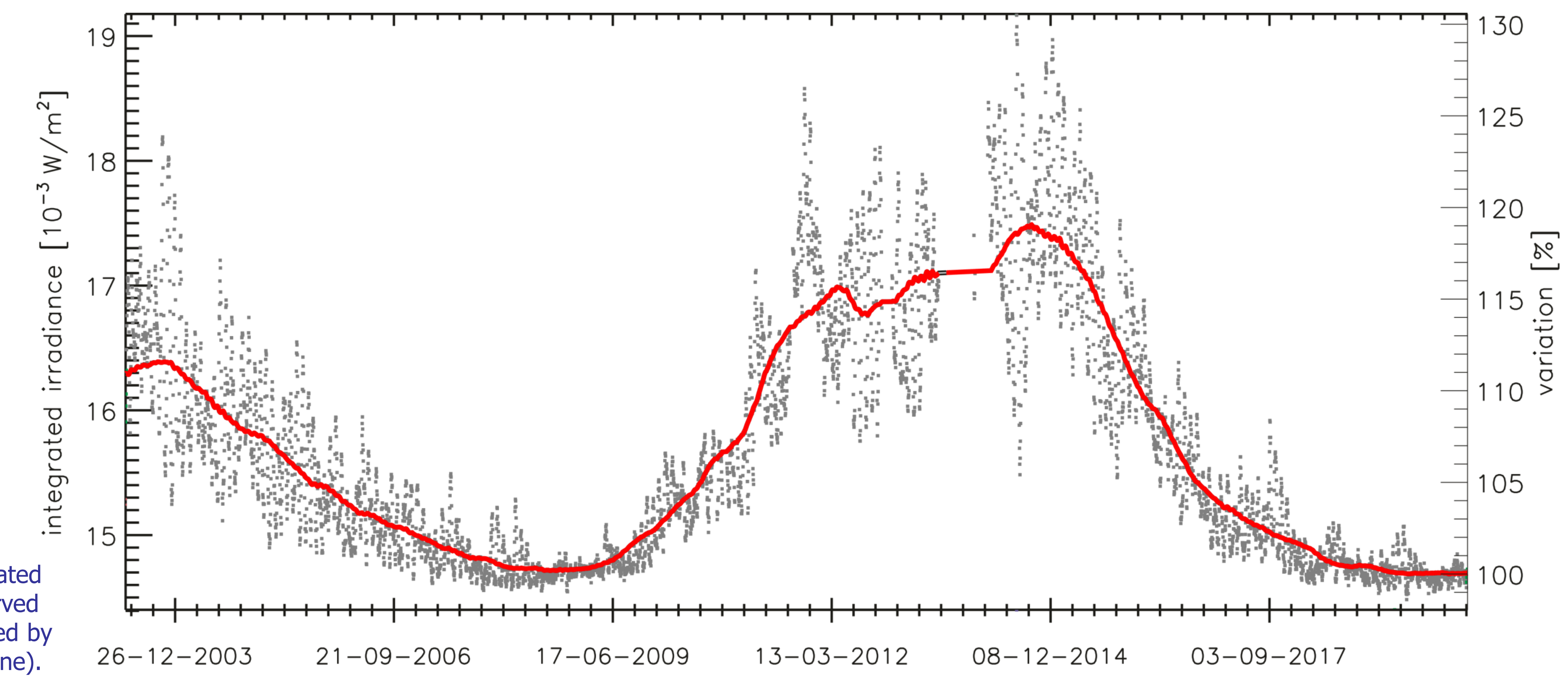

Fig. 9. The variation of the Mg II k integrated irradiance during the solar cycle as observed by SORCE/SOLSTICE (grey dots) smoothed by the running average over 400 days (red line).

References

Curdt, Tian, Teriaca, Schühle, Lemaire 2008, A&A 492, L9
Gunár, Schwartz, Koza, Heinzel 2020, A&A 644, A109
Gunár, Koza, Schwartz, Heinzel, Liu 2021a, ApJS 255, 16
Gunár, Heinzel, Schwartz, Koza 2021b, ApJ, in preparation
Heinzel and Anzer 2001, A&A 375, 1082
Koza, Gunár, Schwartz, Heinzel, Liu 2021, ApJ, in preparation
Machol, Snow, Woodraska, et al. 2019, Earth & Space Sci. 6, 2263
Wilhelm, Lemaire, Curdt, et al. 1997, Solar Phys. 170, 75

Acknowledgements

S.G. and P.H. acknowledge support from the grant No. 19-16890S and grant No. 19-17102S of the Czech Science Foundation (GA R). S.G. acknowledges support from the grant No. 19-20632S of the Czech Science Foundation. S.G., P.S., P.H. and J.K. acknowledge support from the Joint Mobility Project SAV-18-03 of Academy of Sciences of the Czech Republic and Slovak Academy of Sciences. P.S. and J.K. acknowledge support from the project VEGA2/0048/20 of the Science Agency. S.G., P.H. and W. L. thank for the support from project RVO:67985815 of the Astronomical Institute of the Czech Academy of Sciences. The authors thank W. Curdt, J.-C. Vial, N. Labrosse, J. Štěpán and M. Pavelková for valuable discussions.